ISSN 1990-7931, Russian Journal of Physical Chemistry B, 2024, Vol. 18, No. 1, pp. 67–82. © Pleiades Publishing, Ltd., 2024.

STRUCTURE OF CHEMICAL COMPOUNDS, QUANTUM CHEMISTRY, SPECTROSCOPY

# Computational Modelling of Boron Nitride Nanosheet for Detecting and Trapping of Water Contaminant

**F. Mollaamin[a, b, *], S. Mohammadi[c], Z. Khalaj[d], and M. Monajjemi[c]**

[a] *Department of Food Engineering, Faculty of Engineering and Architecture, Kastamonu University, Kastamonu, Turkey*

[b] *Department of Biology, Faculty of Science, Kastamonu University, Kastamonu, Turkey*

[c] *Department of Chemical Engineering, Central Tehran Branch, Islamic Azad University, Tehran, Iran*

[d] *Department of Physics, Shahr-e-Qods Branch, Islamic Azad University, Tehran, Iran*

**e-mail: smollaamin@gmail.com*

Received July 3, 2023; revised September 8, 2023; accepted October 20, 2023

**Abstract**—Boron nitride (BN) is environment friendly chemical compound extracted from identical numbers of boron (B) and nitrogen (N) atoms. This research wants to evaluate the efficiency of BN nanosheet for removing of water contaminant. The changes of charge density (Q) have shown a more important charge transfer toward BN nanosheet which acts as the electron acceptor while $CH_3OH$, $CHBr_2$, NaOH and $NH_3$ molecules act as the electron donors. Based on nuclear quadrupole resonance analysis, BN nanosheet represent s enough capability for adsorbing $CH_3OH$, $CHBr_2$, NaOH and $NH_3$ through electric potential values of hydrogen, carbon, nitrogen, oxygen, bromine and boron atoms during adsorption of organic molecule (adsorbate) on BN nanosheet (adsorbent). Besides, NMR spectroscopy exhibited the remarkable peaks around carbon, nitrogen, oxygen and bromine atoms through the adsorption procedure of $CH_3OH$, $CHBr_2$, NaOH and $NH_3$ on the BN nanosheet with the fluctuations in the chemical shielding behaviors of isotropic and anisotropy attributes. All the measured thermodynamic parameters extracts from IR spectrums have exhibit the most stability energy for $CHBr_2$ and $CBr_2$–BN. This work can evaluate the adsorption of different organic contaminants of $CH_3OH$, $CHBr_2$, NaOH and $NH_3$ on the BN-based nanosheet and correspondingly can introduce helpful information for using this nanomaterial in water treatment.

**Keywords:** BN nanosheet, $CH_3OH$, $CHBr_2$, NaOH, $NH_3$, DFT, water treatment, Langmuir adsorption

**DOI:** 10.1134/S1990793124010330

## INTRODUCTION

These BN structures have special physical, structural, and chemical characteristics such ass wide surface area per unit mass, thermal and chemical stability, UV photoluminescence, insulation properties, large band gap, high conductivity, and exceptional oxidation resistance. These characteristics make BNs potential substance for their utility in different fields like sensor applications, pollutants removal and treatment, hydrogen energy storage, and heterogeneous catalysis [1, 2].

A variety of organic and inorganic and pollutants containing pharmaceuticals, endocrine-disrupting compounds, dye chemicals which are usually separated into organic-inorganic and synthetic -natural groups, and heavy metals such as Cu, Cr, Zn, Ni, Pb, Hg, Cd, As, and Ag have often been discovered in many drinking water sources and wastewaters worldwide [3–6].

Semiconductor materials are mainly prepared from the elements in groups II to VI of the periodic table [7]. The compound in the group III–V, each atom of group III is bonded to four atoms of group V for attaining an octet in the valence band, when the valence charge from an atom of group V transfers toward an atom of group III and cultivates partial ionic bonding to the crystal surface [8–11].

Various methods have been applied to remove different inorganic and organic pollutants in water consisting of chemical precipitation, photocatalytic oxidation, membrane filtration, coagulation, ion exchange, and adsorption [12–15]. Adsorption is one of the most generally employed removal methods due to its special traits like selectivity, simplicity, and cost-efficiency [16–20].

Recently, 2D or 3D nanomaterials with unique specifications have been investigated as engaged adsorbents for the impressive cure of different environmental chemicals such as carbon nanotubes, graphene surfaces, Metal–Organic Frameworks (MOFs), and boron nitrides with thin shapes, principal specific surface area and powerful functional situations [21–25].

**Table1.** The characteristic of $CH_3OH$, $CHBr_2$, NaOH, $NH_3$ structures after adsorption on the BN nanosheet

| Compound | Bader charge (e) | $\Delta Q_t = Q_2 - Q_1$ | Bond length | |
|---|---|---|---|---|
| $CH_3OH$ | –0.292 | +0.033 | O → B ($CH_3O$–BN) | 1.55 Å |
| $CHBr_2$ | –0.325 | 0 | C → B ($CBr_2$–BN) | 1.59 Å |
| NaOH | –0.298 | +0.027 | O → B (OH–BN) | 1.53 Å |
| $NH_3$ | –0.396 | –0.071 | N → B ($NH_2$–BN) | 1.57 Å |

Boron nitride nanomaterials have been used owing to their unique characteristics such as eco-friendly attributes for pollutant adsorption, big surface area, high chemical and mechanical strength and semiconducting property [26–28]. Boron nitride nanometerials usually exhibits semi-leading behavior, which is considered a proper alternative to carbon nanotubes. The properties of boron and nitrogen atoms which are the first neighbors of carbon in the periodic table, make Boron nitride as an interesting subject of numerous studies [29–34].

In the recent years, different researches on the adsorption of chemical contaminants and applying various boron nitride nanomaterials as adsorbents for water purification have been studied [35–48]. Various physical shapes of boron nitride (BN)-based nano adsorbents such as nanoparticles, fullerenes, nanotubes, nanofibers, nanoribbons, nanosheets, nanomeshes, nanoflowers, and hollow spheres have been broadly considered possible adsorbents owing to their exceptional characteristics such as large surface area, structural variability, great chemical/mechanical strength, abundant structural defects, high reactive sites, and functional groups [49–51]. Particularly, this research work aims to assess the influences of adsorbent properties of boron nitride (BN) nanosheet (charge transfer, electromagnetic and thermodynamic, surface area, and functional group) on contaminant removal, and examine the removal of selected contaminants of $CH_3OH$, $CHBr_2$, NaOH and $NH_3$ during the adsorption process.

## MATERIALS AND METHOD

The adsorption sites for a typical single-layered BN material are accessible on both sides of the BN. However, large-scale manufacturing of single-layered BN nanosheets is complicated through the parameters like structural stability and oxidation resistance. Moreover, multilayer BN nanosheets have efficient potential for removing the heavy metal pollutants in the aqueous medium. In fact, adsorption of contaminants applying BN materials deal with a physicochemical interaction present at BN–water interface due to its high surface zone per unit mass and surface-active attributes.

The Perdew–Burke–Ernzerhof (PBE) functional with high-precision generalized gradient approximation (GGA) is applied to simulate the theoretical system by GaussView 6.06.16 [52] and Gaussian 16, Revision C.01 [53] due to density functional theory (DFT) [54]. Figure 1 indicates the adsorption of water contaminants of $CH_3OH$, $CHBr_2$, NaOH or $NH_3$ molecules on the BN nanosheet.

The charge transfer between adsorbates of $CH_3OH$, $CHBr_2$, NaOH and $NH_3$ and adsorbent of BN nanosheet is calculated due to the Bader charge analysis [55]. This method can measure charge accumulation from the charge of each atom in the complex model. Finally, the total adsorption charge transfer can be obtained as formula: $\Delta Q_t = Q_2 - Q_1$, where $Q_1$ and $Q_2$ remark the charge distribution of $CH_3OH$, $CHBr_2$, NaOH and $NH_3$ on the BN surface before and after adoption, respectively. As a matter of fact, positive $\Delta Q_t$ indicates that electrons are transferred from $CH_3OH$, $CHBr_2$, NaOH and $NH_3$ to the surface of BN nanosheet, and the adsorbent acts as an electron acceptor [56, 57].

The adsorbing of $CH_3OH$, $CHBr_2$, NaOH and $NH_3$ molecules on the surface of BN nanosheet was defined by the theory Langmuir isotherm [58–61]. The adsorbates of $CH_3OH$, $CHBr_2$, NaOH and $NH_3$ molecules are maintained on surface of BN with "Langmuir" chemisorption (Fig. 1).

The changes of charge density analysis in the adsorption process has illustrated that BN nanosheet shows the Bader charge of before adsorption of $CH_3OH$, $CHBr_2$, NaOH, $NH_3$ and after adsorption of these molecules, respectively. Therefore, the changes of charge density for Langmuir adsorption of $CH_3OH$, $CHBr_2$, NaOH, $NH_3$ on BN surface alternatively are $\Delta Q_{CH_3OH@BN} > \Delta Q_{NaOH@BN} > \Delta Q_{CHBr_2@BN} > \Delta Q_{NH_3@BN}$ (Table 1).

The values of changes of charge density have shown a more important charge transfer for BN nanosheet which acts as the electron acceptor while $CH_3OH$, $CHBr_2$, NaOH, $NH_3$ molecules act as the stronger electron donors through adsorption on the graphitic-like BN surface.

For calculating the adsorption energy, the total energy of the $CH_3OH$, $CHBr_2$, NaOH, $NH_3$ molecules and BN surface should be computed. Then, it has been tailored the spin-polarized DFT calculation

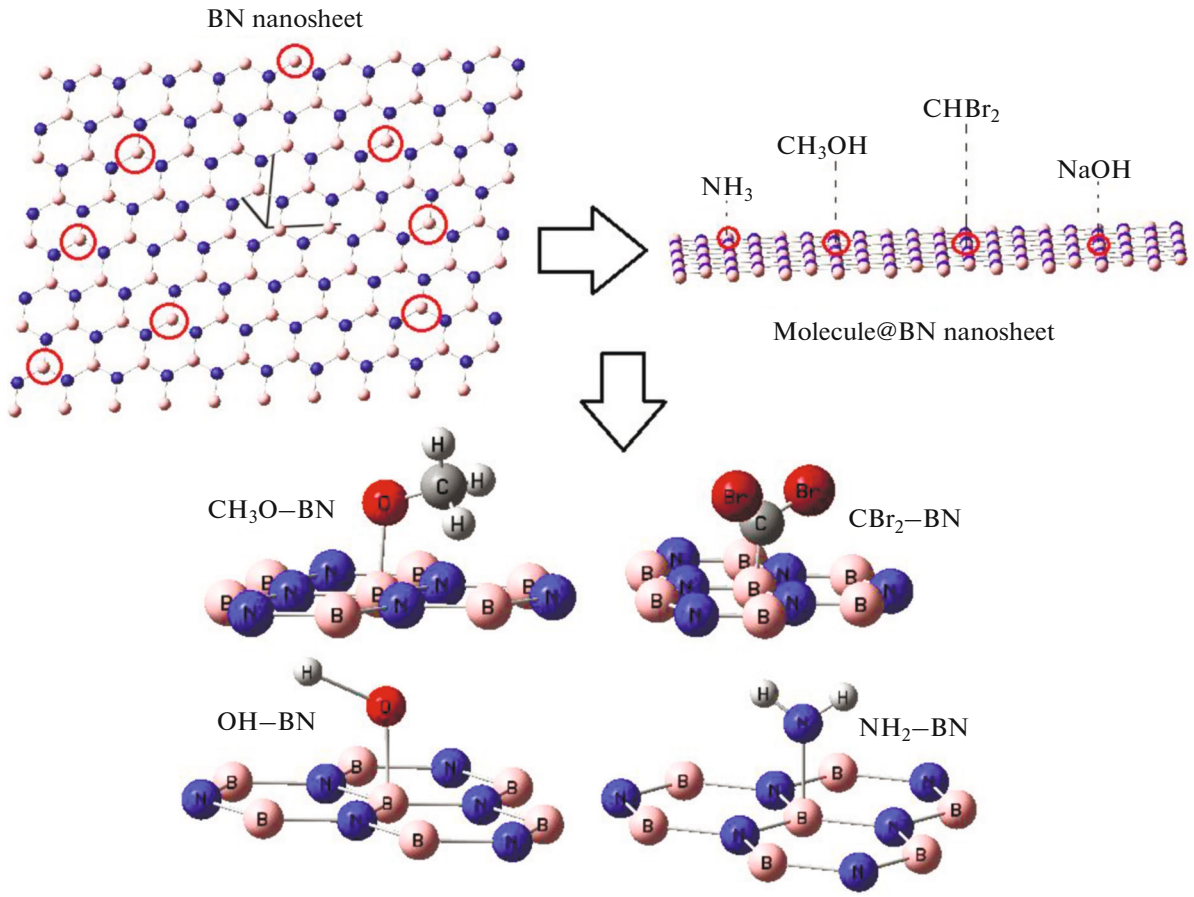


**Fig. 1.** The schematic of the Langmuir adsorption of $CH_3OH$, $CHBr_2$, NaOH and $NH_3$ molecules onto BN nanosheet based on optimized coordination towards formation of $CH_3O$–BN, $CBr_2$–BN, OH–BN and $NH_2$–BN complexes, respectively.

with ONIOM model [62–66] accompanying the same force and energy convergence accuracy to the adsorption systems, with CAM-B3LYP [67] functional and with 6-311+G(*d*, *p*) [68] basis set for hydrogen, carbon, nitrogen, oxygen, bromine and LANL2DZ for boron in the adsorption site for the first layer (high level). Second layer (medium level) has been considered on some boron and nitrogen atoms of BN nanosheet in the adsorption site due to semi-empirical methods. The third layer (low level) has been saved on the remained boron and nitrogen atoms of BN nanosheet with molecular mechanic force fields (Fig. 1) [62] as formula:

$$E_{\mathrm{ONIOM}} = E_{\mathrm{1st}} + E_{\mathrm{2nd}} + E_{\mathrm{3rd}}. \quad (1)$$

To determine the most sensitive structure of BN nanosheet as the selective sensor for detecting gas molecules of $CH_3OH$, $CHBr_2$, NaOH and $NH_3$, the binding energy of each system has been calculated. Therefore, we have found that the priority for selecting the surface binding of O-atom of the $CH_3O$–BN and OH–BN, N-atom of $NH_2$–BN and C–atom of $CBr_2$–BN complexes in adsorption site can be impacted by the existence of close atoms in the BN surface. The simulated distribution functions of $CH_3O$–BN, $CBr_2$–BN, OH–BN and $NH_2$–BN complexes have illustrated that the created clusters lead to the bond lengths of O → B in $CH_3O$–BN, O → B in OH–BN, N → B in $NH_2$–BN, and C → B in $CBr_2$–BN (Table 1).

## RESULTS AND DISCUSSION

As the BN nanosheet possess magnetic characteristics so can accomplish fast separation of pollutants as well as quickly recover after treatment under the influence of a magnetic field, it was considered for adsorption of water pollutants including $CH_3OH$, $CHBr_2$, NaOH and $NH_3$ molecules.

These experiments have been accomplished using spectroscopy analysis through some physical and chemical properties of optimized structures of initial compounds and products through Langmuir adsorption mechanism.

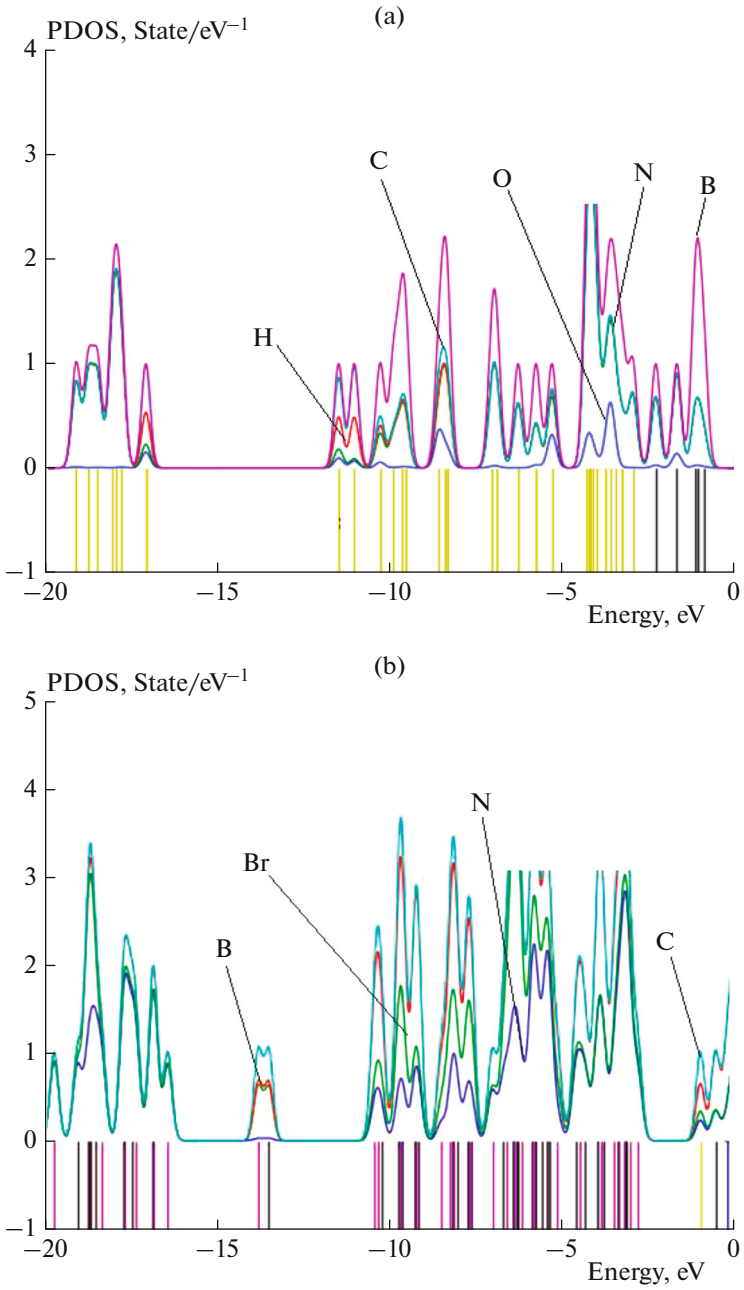


**Fig. 2.** PDOS adsorption of $CH_3OH$, $CHBr_2$, NaOH and $NH_3$ molecules onto BN nanosheet towards formation of (a) $CH_3O$–BN, (b) $CBr_2$–BN, (c) OH–BN and (d) $NH_2$–BN, respectively.

The electronic structures of $CH_3OH$, $CHBr_2$, NaOH and $NH_3$ adsorbed on the BN nanosheet have been analyzed to simplify subsequent discussion for interfacial electronic properties using CAM-B3LYP/LANL2DZ, 6-311+G(*d*, *p*) basis sets. The graph of partial DOS (PDOS) has illustrated that the *p* states of the adsorption of N–, O– and C– on the BN nanosheet are dominant through the conduction band (Figs. 2a–2d). Moreover, the existence of covalent features for these complexes has exhibited the identical energy amount and figure of the PDOS for the *p* orbitals of N, O, C and *d* orbitals of Br (Figs. 2a–2d).

Figures 2a–2d shows that the $CH_3O$–, $CBr_2$–, OH–, and $NH_2$– states of $CH_3O$–BN, $CHBr_2$–BN, OH–BN and $NH_2$–BN nanosheets, respectively, have more contribution at the middle of the conduction band between –5 to –10 eV. Contribution of boron, carbon and nitrogen states are expanded and close together, but oxygen states have minor contributions in $CH_3O$–BN sheet (Fig. 2a). In $CHBr_2$–BN

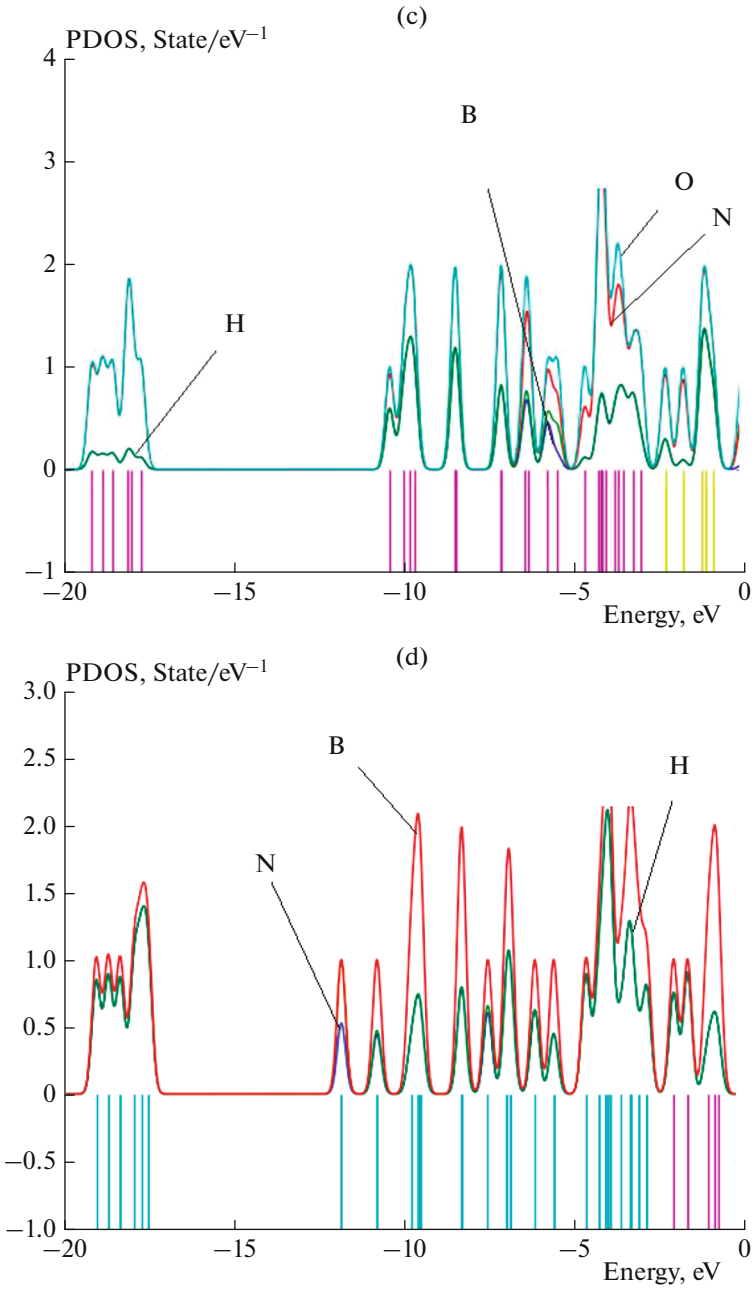


**Fig. 2.** (Contd.)

sheet, contributions of nitrogen and oxygen states are expanded and close together, but nitrogen and bromine states have minor contributions (Fig. 2b). In OH–BN sheet, contributions of boron and carbon states are expanded and close together, but hydrogen and boron states have minor contributions (Fig. 2c). In addition, in $NH_2$–BN sheet, contributions of hydrogen and boron states are expanded and close together, but nitrogen states have minor contributions (Fig. 2d).

The results also approved by the partial electron density (PDOS) which have showed a certain charge association between BN nanosheet and water pollutant molecules of $CH_3OH$, $CHBr_2$, NaOH and $NH_3$.

Nuclear Quadrupole Resonance (NQR) is a straight frame of the interaction of the quadrupole moment with the electric field gradient (EFG) which is produced by the electronic structure of its ambiance [69–72]. In this research work, the electric potential as the quantity of work energy through carrying over the electric charge from one position to another position

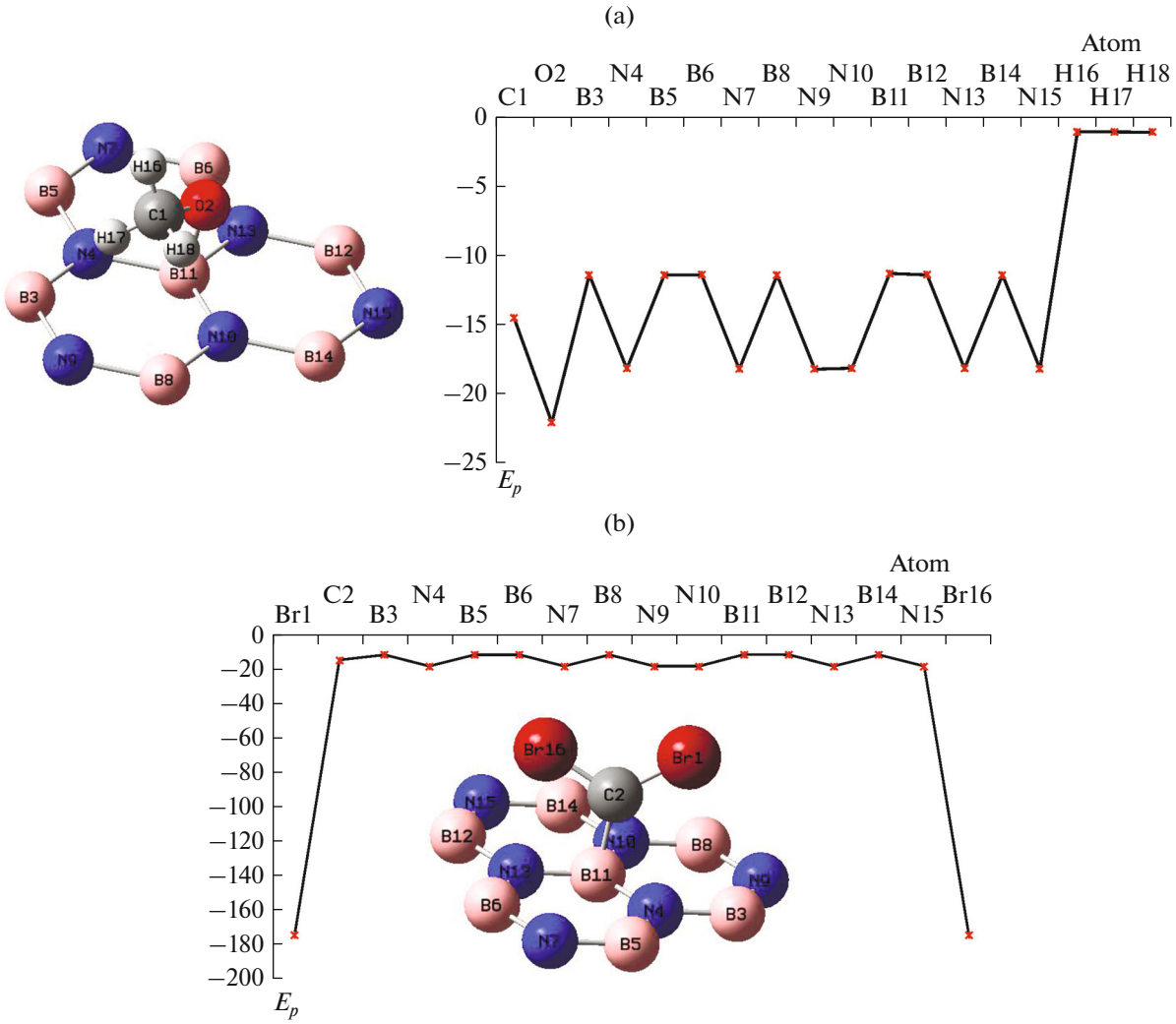


**Fig. 3.** The electric potential versus Bader charge through NQR calculation for adsorption clusters of (a) $CH_3O$–BN, (b) $CBr_2$–BN, (c) OH–BN and (d) $NH_2$–BN using CAM-B3LYP/EPR-III, LANL2DZ,6-31+G(*d*, *p*).

in the essence of electric field has been evaluated for $CH_3O$–BN, $CBr_2$–BN, OH–BN and $NH_2$–BN complexes using CAM-B3LYP/EPR-III,LANL2DZ, 6-31+G(*d*, *p*) level of theory (Fig. 3).

Furthermore, in Figs. 3a–3d, it has been sketched the electric potential of nuclear quadrupole resonance for some atoms of hydrogen, boron, carbon, nitrogen, oxygen and bromine in the adsorption process of $CH_3OH$, $CHBr_2$, NaOH and $NH_3$ molecules adsorbed on the BN nanosheet which have been calculated by CAM-B3LYP/EPR-III, 6-311+G(*d*, *p*), LANL2DZ.

In Fig. 3, it has been remarked the changes of electric potential for hydrogen, boron, carbon, nitrogen, oxygen and bromine in the active site of Langmuir adsorption. In fact, it has been observed the effect of the binding between C, N, and O with boron in the BN nanosheet during adsorbing $CH_3OH$, $CHBr_2$, NaOH and $NH_3$ molecules through resulted electric potential using NQR analysis with relation coefficients of $R^2 = 0.9423$ for $CH_3O$–BN (Fig. 3a), $R^2 = 0.9525$ for $CBr_2$–BN (Fig. 3b), $R^2 = 0.9804$ for OH–BN (Fig. 3c), and $R^2 = 0.9533$ for $NH_2$–BN (Fig. 3d). It's obvious that the capability of BN nanosheet for detecting of $CH_3OH$, $CHBr_2$, NaOH and $NH_3$ molecules is fluctuated by their selectivity and sensitivity which can represent the efficiency of these surfaces as the promising sensors.

Isotropic ($\sigma_{iso}$) and anisotropy ($\sigma_{aniso}$) shielding tensors of "NMR" spectroscopy for certain atoms in the active site of $CH_3OH$, $CHBr_2$, NaOH and $NH_3$ adsorbed on the BN nanosheet through the formation of the binding between gas molecules and solid surfaces are calculated using Gaussian 16, Revision C.01 [53, 73–76].

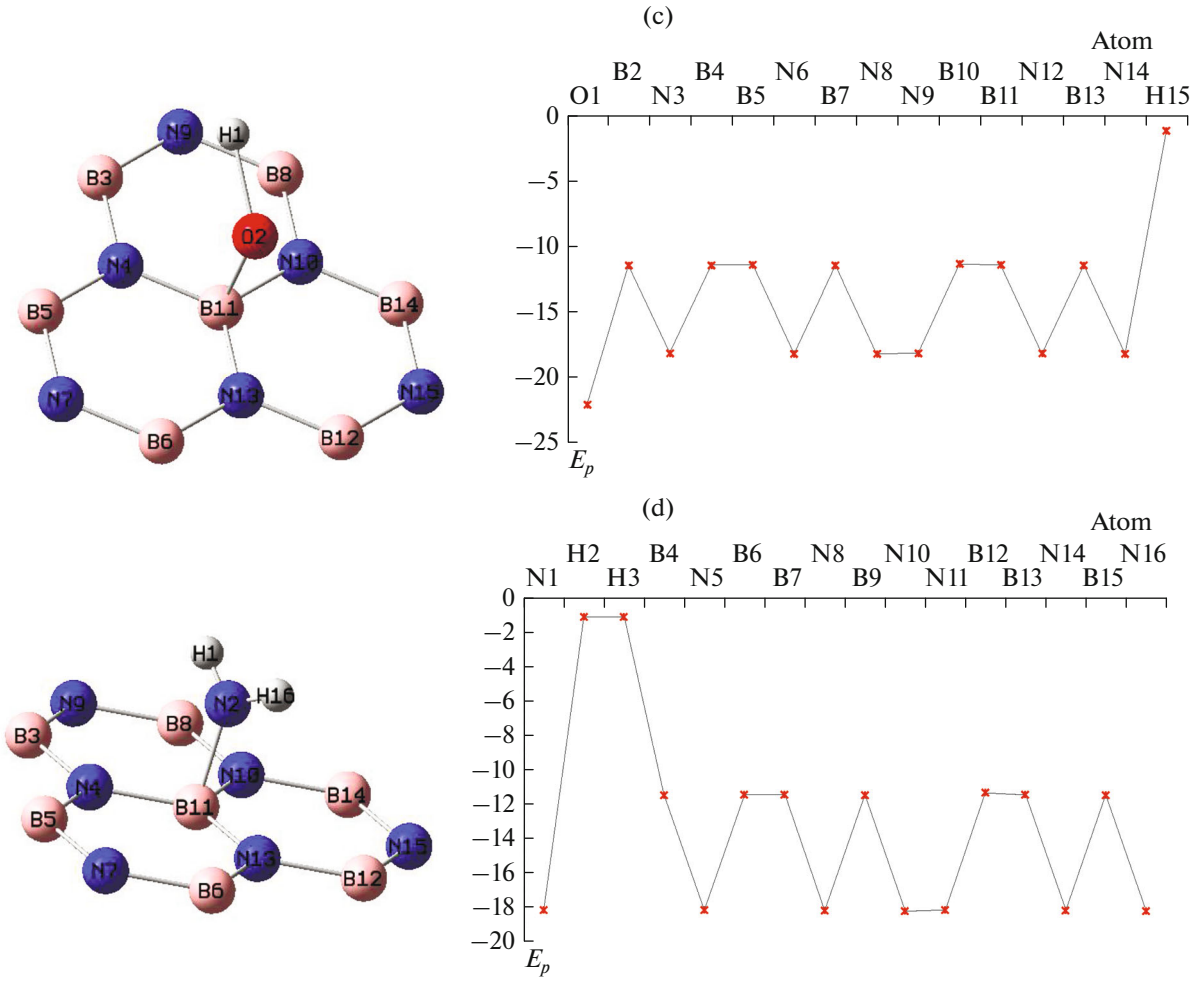


**Fig. 3.** (Contd.)

In Figs. 4a–4d, NMR data indicates the notable amounts for $CH_3OH$, $CHBr_2$, NaOH and $NH_3$ which have been doped on the BN nanosheet. In fact, the adsorption of $CH_3OH$, $CHBr_2$, NaOH and $NH_3$ introduces spin polarization on the BN nanosheet which indicates that this surface might be applied as magnetic carbon, nitrogen and oxygen detectors. In fact, it is revealed that the isotropic and anisotropy shielding augment with the occupancy in $CH_3OH$, $CHBr_2$, NaOH and $NH_3$ penetrated by C-, N-, O-atoms in $CH_3O$–BN (O → B), $CBr_2$–BN (C → B), OH–BN (O → B ) and $NH_2$–BN(N → B) (Figs. 4a–4d).

The resulted graphs of NMR data in Figs. 4a–4d have shown approximately the identical chemical shielding behavior of isotropic and anisotropy factors for $CH_3O$–BN, OH–BN and $NH_2$–BN with several sharp peaks related to nitrogen atoms involving the adsorption site including (N7, N9, N15) (Fig. 4a), (N6, N8, N14) (Fig. 4c), and (N5, N8, N10) (Fig. 4d).

However, has been shown $CBr_2$–BN with two sharp peaks related to boron and carbon atoms involving the adsorption site including (B16 and C2) (Fig. 4b).

Although, in the NMR spectroscopy, it has been observed the remarkable peaks around carbon, nitrogen, oxygen and bromine atoms through the adsorption procedure of $CH_3OH$, $CHBr_2$, NaOH and $NH_3$ on the BN nanosheet, there are some fluctuations in the chemical shielding behaviors of isotropic and anisotropy attributes.

In this part, the stability of complexes including water pollutant of $CH_3OH$, $CHBr_2$, NaOH and $NH_3$ adsorbed on the boron nitride (BN) nanosheet has been investigated through thermodynamic properties which define the reactions that $CH_3OH$, $CHBr_2$, NaOH and $NH_3$ endure in the boron coordination sphere. Concerning adsorption process, the thermodynamic characters were evaluated for $CH_3OH$, $CHBr_2$, NaOH and $NH_3$ and complexes of $CH_3O$–

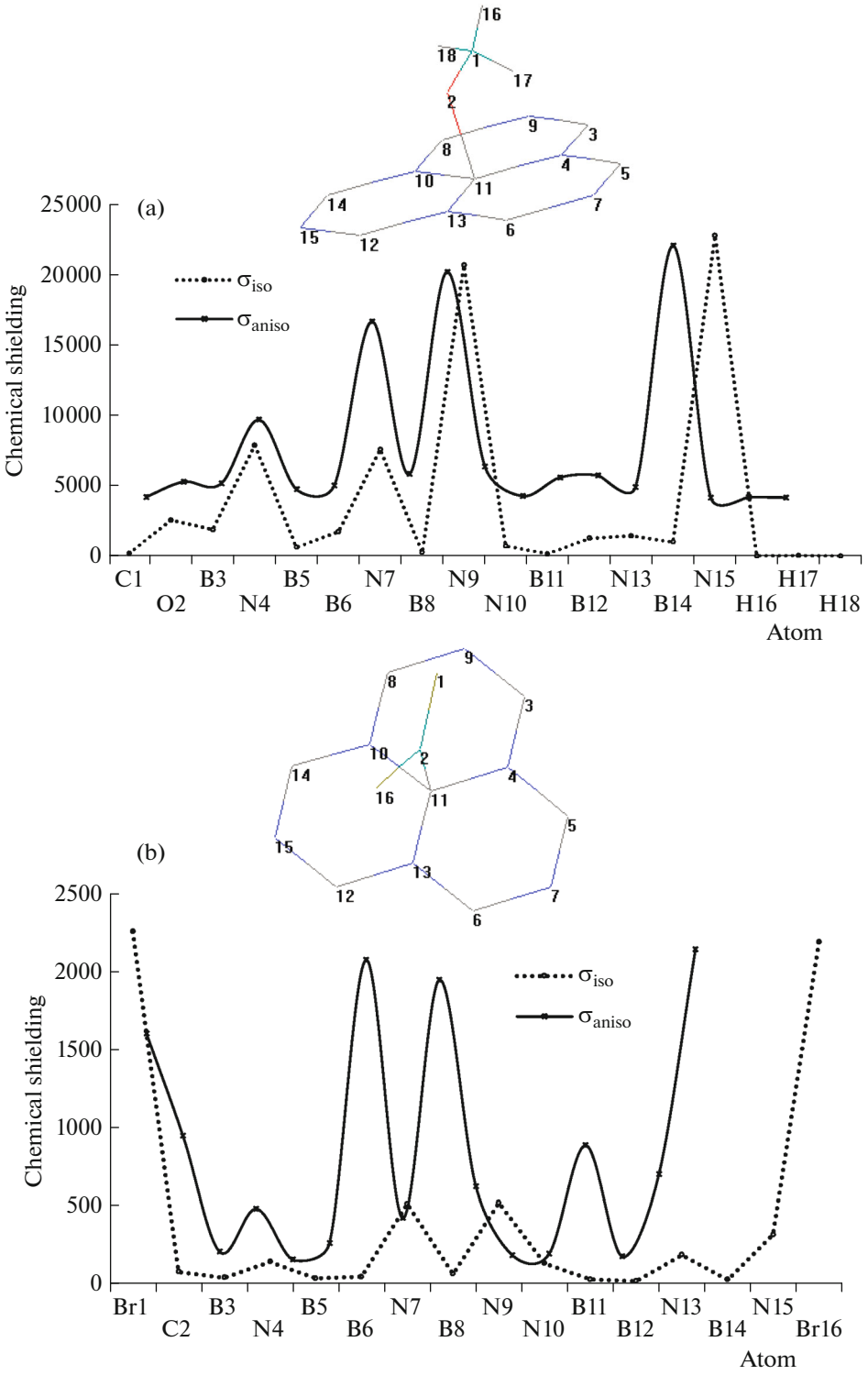


**Fig. 4.** NMR adsorbing of $CH_3OH$, $CHBr_2$, NaOH and $NH_3$ through adsorption on BN nanosheet through production of (a) $CH_3O$–BN, (b) $CBr_2$–BN, (c) OH–BN and (d) $NH_2$–BN using CAM-B3LYP/EPR-III, LANL2DZ,6-31+G(*d*, *p*).

BN, $CBr_2$–BN, OH–BN and $NH_2$–BN on the surface of BN nanosheet as the water pollutant detectors which can be applicable as the selective sensors for these compounds removal (Table 2).

Furthermore, the IR spectrums for adsorption of $CH_3OH$, $CHBr_2$, NaOH and $NH_3$ on the surface of the boron nitride (BN) nanosheet have been reported in Fig. 5.

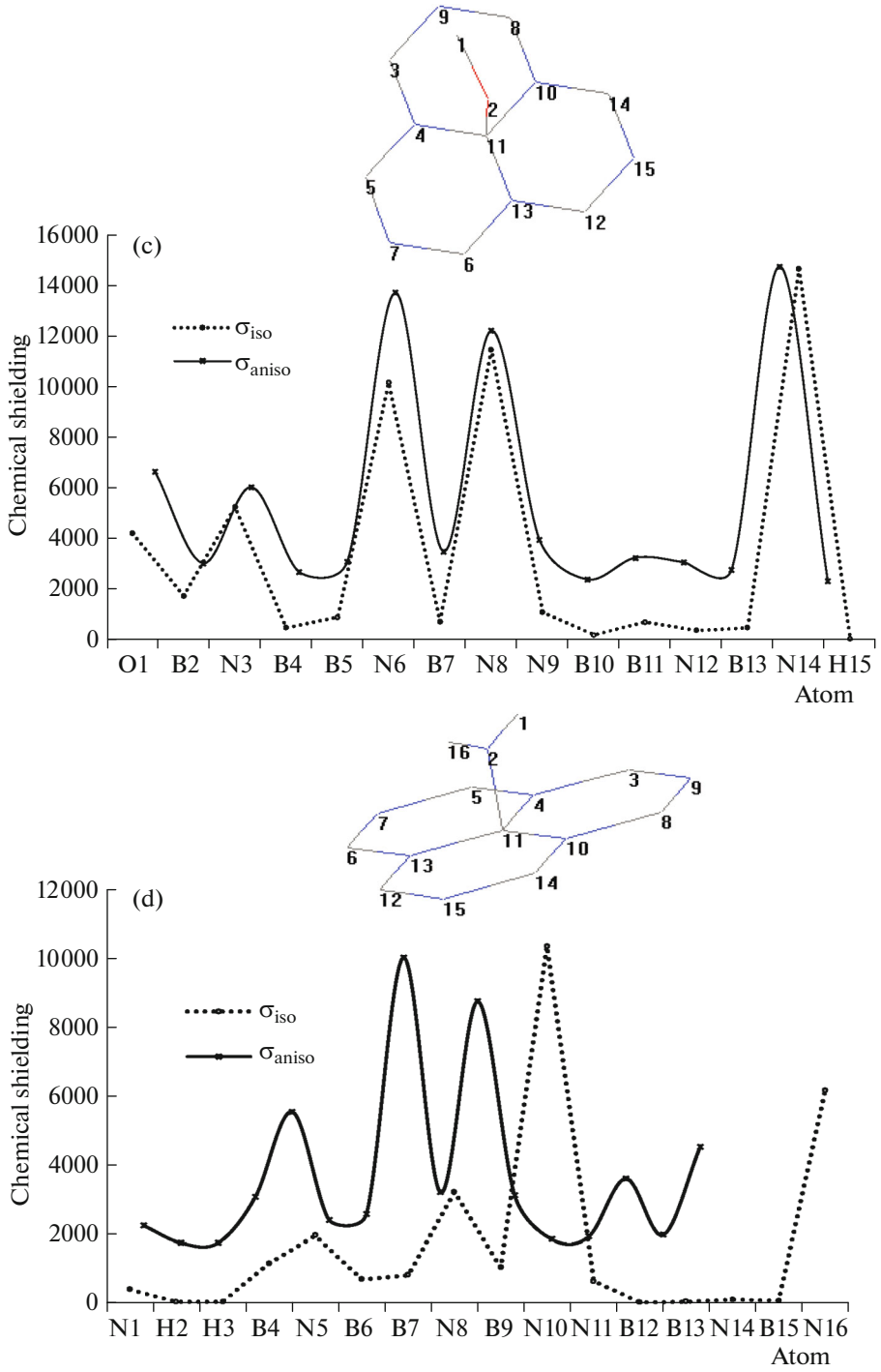


**Fig. 4.** (Contd.)

The graphs of Fig. 5a have been observed in the frequency range between 100–700 $cm^{-1}$ for the BN nanosheet. Figure 5b has shown frequency range between 100–3500 $cm^{-1}$ for $CH_3O$–BN complex with a sharp peak in around 250 $cm^{-1}$. Figures 5c and 5d have the similar fluctuation of frequency between 100–1000 $cm^{-1}$ for $CBr_2$–BN (Fig. 5c) with several sharp peaks around 450, 650, 950 $cm^{-1}$ and for OH–BN (Fig. 5d) with several sharp peaks around 200, 270, 420 $cm^{-1}$, respectively. Moreover, $NH_2$–BN has remarked a considerable frequency peak about 3850 $cm^{-1}$ (Fig. 5e).

In addition, the high amounts of the Langmuir adsorption isotherm graphs based on relative adsorp-

**Table 2.** The thermodynamic character of $CH_3OH$, $CHBr_2$, NaOH and $NH_3$ adsorbed on the BN nanosheet as the selective water pollutant sensors

| Compound | $\Delta H^\circ \times 10^{-4}$, kcal/mol | $\Delta G^\circ \times 10^{-4}$, kcal/mol | $S^\circ$, cal/K mol | Dipole moment (Debye) |
|---|---|---|---|---|
| BN nanosheet | −31.0214 | −31.0238 | 103.077 | 0.4110 |
| $CH_3OH$ | −7.1568 | −7.1584 | 55.576 | 1.3748 |
| $CHBr_2$ | −321.9162 | −321.9183 | 71.878 | 0.8932 |
| NaOH | −14.7376 | −14.7393 | 56.923 | 6.6903 |
| $NH_3$ | −3.4958 | −3.4973 | 48.843 | 1.6650 |
| $CH_3O$-BN | −38.1324 | −38.1355 | 104.117 | 1.3507 |
| $CBr_2$−BN | −352.9039 | −352.9075 | 120.009 | 2.2734 |
| OH−BN | −35.6875 | −35.6907 | 106.940 | 1.7390 |
| $NH_2$−BN | −34.4705 | −34.4736 | 104.137 | 1.0754 |

**Table 3.** LUMO (eV), HOMO (eV), and band energy gap ($\Delta E$ /eV) of $CH_3O$−BN, $CBr_2$−BN, OH−BN and $NH_2$−BN complexes

| Water pollutant → BN_sh | HOMO | LUMO | $\Delta E = E_{LUMO} - E_{HOMO}$ |
|---|---|---|---|
| $CH_3O$−BN_sh | −2.9456 | −2.2789 | 0.6667 |
| $CBr_2$−BN_sh | −2.7060 | −0.8914 | 1.8146 |
| OH−BN_sh | −3.0106 | −2.2822 | 0.7284 |
| $NH_2$−BN_sh | −2.8172 | −2.0321 | 0.7851 |

tion energy ($\Delta G^\circ_{ads}$) has been evaluated for interactions between $CH_3OH$, $CHBr_2$, NaOH and $NH_3$ on the surface of BN nanosheet with $R^2 = 0.873$ (Fig. 6).

The adsorptive capacity of $CH_3OH$, $CHBr_2$, NaOH and $NH_3$ on the surface of BN nanosheet is approved by the $\Delta G^\circ_{ads}$ amounts as formula:

$$\Delta G^\circ_{ads} = \Delta G^\circ_{X \to BN\_sh} - \left(\Delta G^\circ_X + \Delta G^\circ_{BN\_sh}\right); \quad (X = CH_3OH,\ CHBr_2,\ NaOH,\ NH_3). \quad (2)$$

Table 2 has shown that the adsorbing of $CH_3OH$, $CHBr_2$, NaOH and $NH_3$ on the surface of BN nanosheet must have both "physical" and "chemical" nature. All the measured relative adsorption energies ($\Delta G^\circ_{ads}$) are almost identical, and exhibit the most stability Gibbs free energy for $CHBr_2$ and $CBr_2$−BN (Fig. 6). In fact, boron sites in BN nanosheet have higher interaction energy from Van der Waals' forces with the molecules of $CH_3OH$, $CHBr_2$, NaOH and $NH_3$ that can make them highly stable.

Furthermore, the results of Table 2 have indicated that $CH_3OH \to BN$, $CHBr_2 \to BN$, NaOH → BN and $NH_3 \to BN$ complexes have the largest gap of Gibbs free energy adsorption with which defines the changes between Gibbs free energy of initial com-

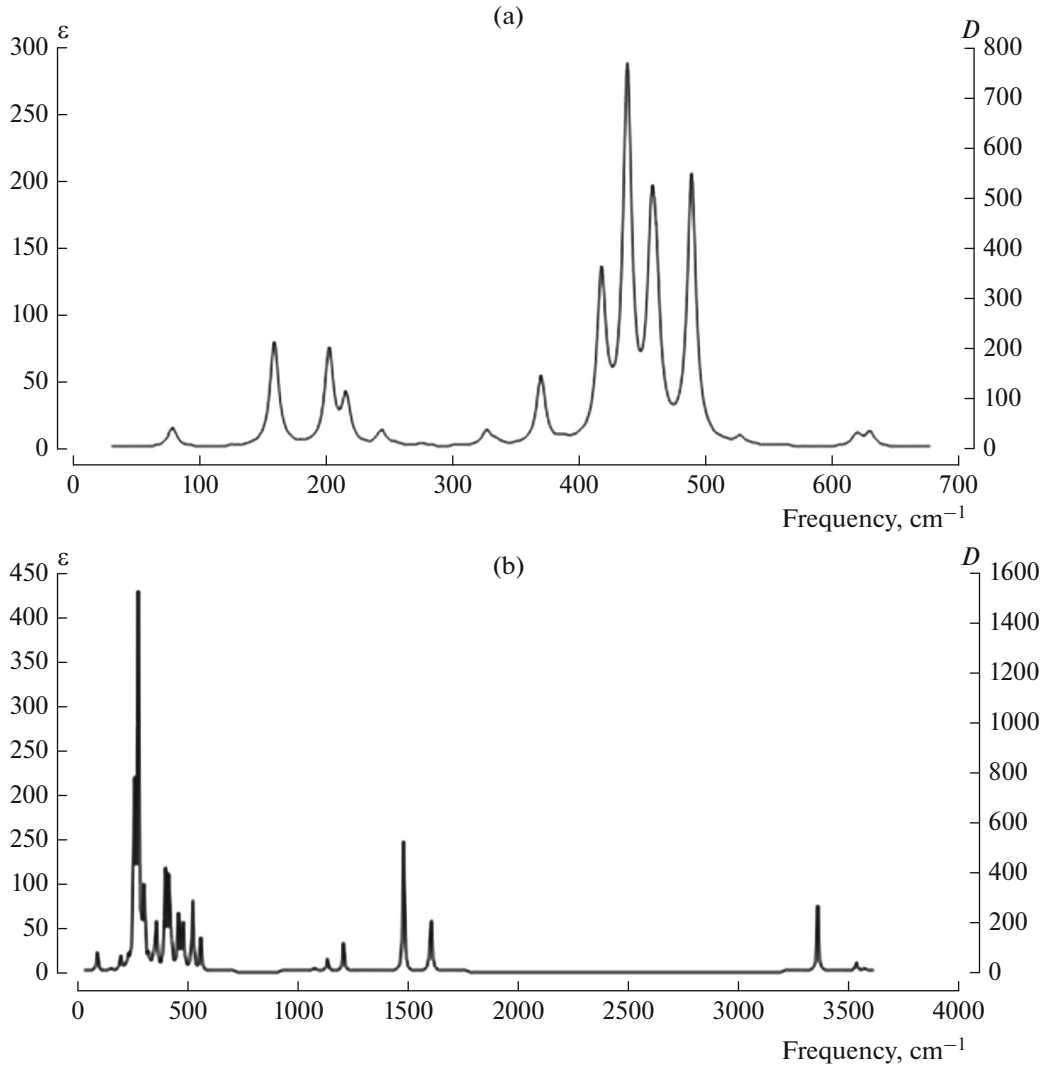


**Fig. 5.** The frequency ($cm^{-1}$) changes through the IR spectrums for (a) BN nanosheet, (b) $CH_3O$–BN, (c) $CBr_2$–BN, (d) OH–BN and (e) $NH_2$–BN complexes.

pounds ($\Delta G^{\circ}_{CH_3OH}$, $\Delta G^{\circ}_{CHBr_2}$, $\Delta G^{\circ}_{NaOH}$, $\Delta G^{\circ}_{NH_3}$) and ($\Delta G^{\circ}_{BN\_sh}$) and product compounds ($\Delta G^{\circ}_{CH_3O-BN}$, $\Delta G^{\circ}_{CBr_2-BN}$, $\Delta G^{\circ}_{OH-BN}$, $\Delta G^{\circ}_{NH_2-BN}$) through polarizability. However, BN nanosheet seems to possess enough efficiency for adsorption water pollutants of $CH_3OH$, $CHBr_2$, NaOH and $NH_3$ through charge transfer from carbon, nitrogen and oxygen to the boron element due to intra-atomic and interatomic interactions.

Based on frontier molecular orbital theory, the lowest unoccupied molecular orbital (LUMO) and Highest Occupied Molecular Orbital (HOMO) and the energy between them are the band gap of the adsorption system was computed. In fact, broad band gap diagram indicates that there is less conductivity [77–80]. The LUMO, HOMO, and band energy gap ($\Delta E$) of $CH_3OH$, $CHBr_2$, NaOH and $NH_3$ on the surface of BN nanosheet as the molecule detector systems denote that the molecule adsorption procedure scatters the electrons of the system (Table 3).

The energy gap between HOMO and LUMO has represented the transporting of molecular electrical characters [81–85]. On the other hand, the difference between HOMO and LUMO has exhibited that the effect of the adsorption process on the electronic behavior of $CH_3OH$, $CHBr_2$, NaOH and $NH_3$ on the surface of BN nanosheet (Table 3).

The illustration of donor–acceptor molecules depends on the relative frontier molecular levels. The HOMO–LUMO gap defines the charge transfer in gas molecules adsorbed on the BN surface through simplified molecular-level diagram. In fact, the amount of transferred charges might be considerably small, as

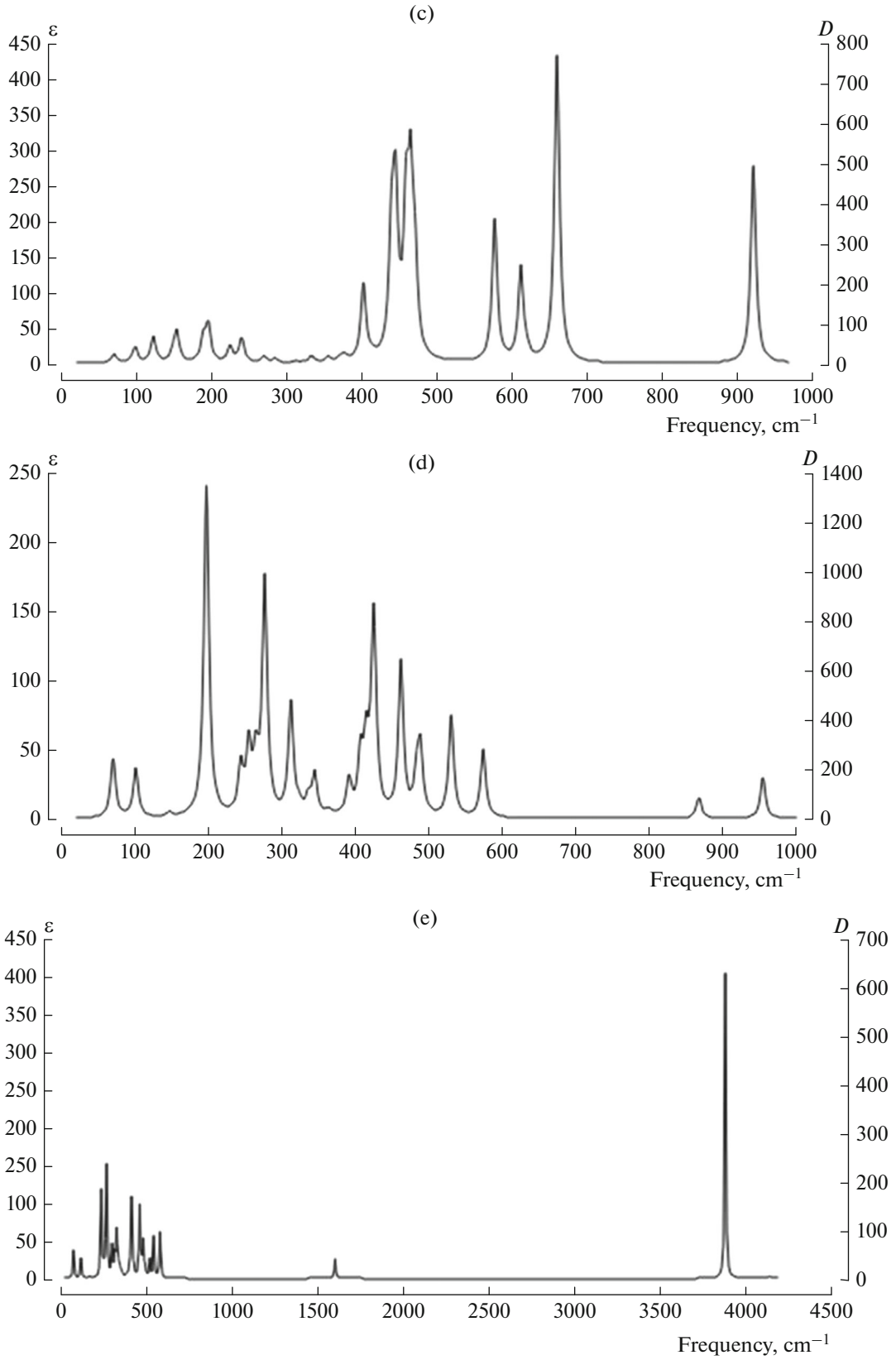


**Fig. 5.** (Contd.)

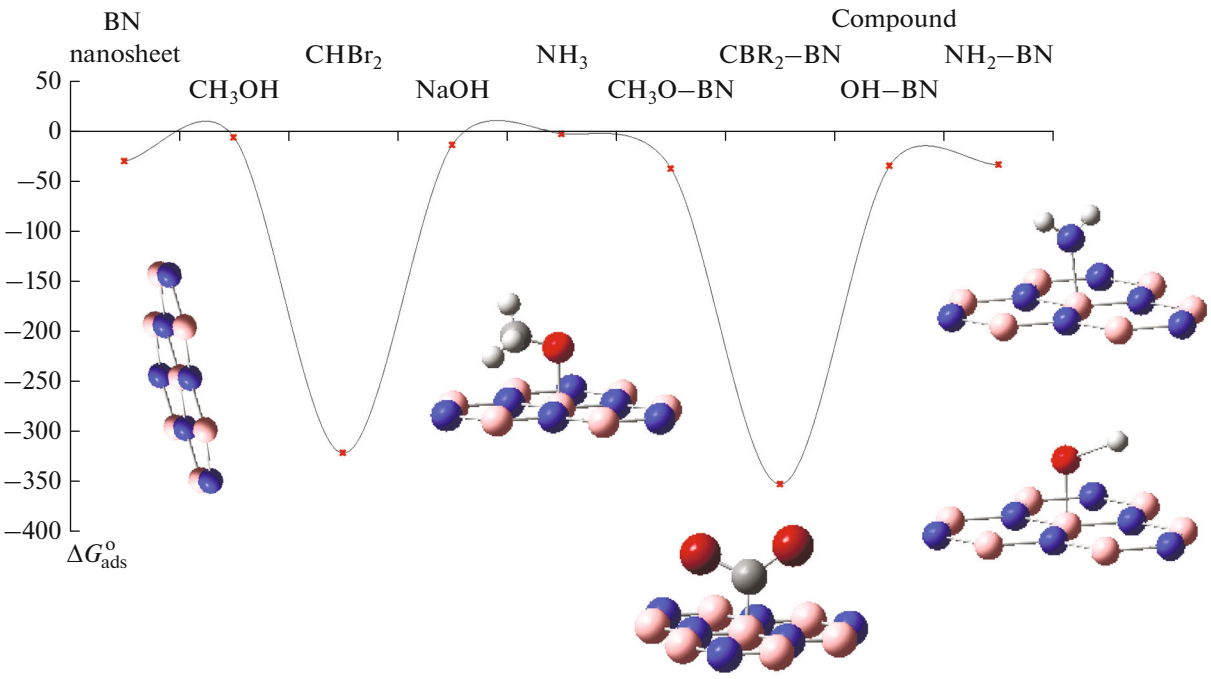


**Fig. 6.** The alterations of adsorption Gibbs free energy ($\Delta G^{\circ}_{ads}$) $CH_3OH$, $CHBr_2$, NaOH and $NH_3$ adsorbed on the BN nanosheet and formation of $CH_3O$–BN, $CBr_2$–BN, OH–BN and $NH_2$–BN complexes.

in the case of parallel and perpendicular coordination, which indicate electronic couplings smaller than in co-facial coordination. The results in Table 3 have indicated the energy level shifts of molecule → surface–HOMO and molecule → surface–LUMO of complexes as a function of their distance *d* orbitals from the high symmetry points of each of $CH_3OH$, $CHBr_2$, NaOH and $NH_3$ molecules adsorbed on the BN surface.

## CONCLUSIONS

Based on the above experiments and analysis, the graphitic-like BN monolayer nanosheet was prepared by a molecular modeling calculation and ONIOM method using DFT study. The adsorption performance and mechanism of BN nanosheet for $CH_3OH$, $CHBr_2$, NaOH and $NH_3$ molecules were investigated.

The current research wanted to remark the illustration of molecule adsorption on BN nanosheet. Particularly, the structural, energetic, and infrared adsorption properties of linearly atop for $CH_3OH$, $CHBr_2$, NaOH and $NH_3$ molecules adsorbing on BN nanosheet has been explored by using DFT calculations.

The values of changes of charge density have shown a more important charge transfer for BN nanosheet which acts as the electron acceptor while organic molecules act as the electron donors through adsorption on the graphitic-like BN surface. It has been assumed that the priority for selecting the surface binding of C-atom of $CHBr_2$, N-atom of $NH_3$, and O-atom of $CH_3OH$ and NaOH in adsorption site can be impacted by the existence of close atoms in the BN surface through formation of $CH_3O$–BN, $CBr_2$–BN, OH–BN and $NH_2$–BN complexes.

In fact, the boron site in BN nanosheet has higher interaction energy from Van der Waals' forces with organic molecules including $CH_3OH$, $CHBr_2$, NaOH and $NH_3$ that can make them highly stable. Finally, our molecular simulation consequences have exhibited the existence of orbital hybridization between boron sites and $CH_3OH$, $CHBr_2$, NaOH and $NH_3$ molecules that also approves the recovery of adsorption susceptibility of BN nanosheet.

This article summarizes the possibility of BN–based nanomaterials as adsorbents for the adsorption of some organic contaminants of $CH_3OH$, $CHBr_2$, NaOH and $NH_3$. The results showed that BN-based nano adsorbents can be a preferable option presently used or studied for water and wastewater treatment.

## ACKNOWLEDGMENTS

In successfully completing this paper and its research, the authors are grateful to Kastamonu University for their support through the office, library, and scientific websites.

## FUNDING

This work was supported by ongoing institutional funding. No additional grants to carry out or direct this particular research were obtained.

## CONFLICT OF INTEREST

The authors of this work declare that they have no conflicts of interest.

## REFERENCES

1. S. Yu, X. Wang, H. Pang, et al., Chem. Eng. J. **333**, 343–360 (2018). https://doi.org/10.1016/j.cej.2017.09.163
2. A. H. Davtyan, Z. O. Manukyan, S. D. Arsentev, et al., Russ. J. Phys. Chem. B **17**, 336–345 (2023). https://doi.org/10.1134/S1990793123020239
3. P. Du, L. Zhang, Y. Ma, et al., Water **12**, 728 (2020). https://doi.org/10.3390/w12030728
4. V. K. Nair, K. Selvaraju, S. Samuchiwal, et al., Processes **11**, 1793 (2023). https://doi.org/10.3390/pr11061793
5. Q. Liu, Y. Cheng, and C. Fan, Sustainability **15**, 8389 (2023). https://doi.org/10.3390/su15108389
6. I. V. Kumpanenko, N. A. Ivanova, O. V. Shapovalova, et al., Russ. J. Phys. Chem. B **16**, 917–925 (2022). https://doi.org/10.1134/S1990793122050050
7. H. Wang, Z. Xie, Z. Zhou, et al., Russ. J. Phys. Chem. B **15**, 949–953 (2021). https://doi.org/10.1134/S1990793121060269
8. G. N. Gerasimov, V. F. Gromov, M. I. Ikim, et al., Russ. J. Phys. Chem. B **15**, 1072–1083 (2021). https://doi.org/10.1134/S1990793121060038
9. L. I. Trakhtenberg, Russ. J. Phys. Chem. B **17**, 600–607 (2023). https://doi.org/10.1134/S1990793123030144
10. A. E. Galashev, Russ. J. Phys. Chem. B **17**, 113–121 (2023). https://doi.org/10.1134/S1990793123010190
11. V. B. Merinov and V. A. Domnin, Russ. J. Phys. Chem. B **17**, 215–221 (2023). https://doi.org/10.1134/S1990793123010268
12. M. V. Grishin, A. K. Gatin, V. A.Kharitonov, et al., Russ. J. Phys. Chem. B **16**, 211–217 (2022). https://doi.org/10.1134/S199079312232001X
13. M. L. Jabbar and K. J. Kadhim, Russ. J. Phys. Chem. B **15**, 46–52 (2021). https://doi.org/10.1134/S1990793121010188
14. C. F. Z. Lacson, M. C. Lu, and Y. H. Huang, Chem. Eng. J. **415**, 128917 (2021). https://doi.org/10.1016/j.cej.2021.128917
15. F. Mollaamin and M. Monajjemi, Russ. J. Phys. Chem. B **17**, 658–672 (2023). https://doi.org/10.1134/S1990793123030223
16. P. O. Oladoye, Chemosphere **287**, 132130 (2022). https://doi.org/10.1016/j.chemosphere.2021.132130
17. L. Joseph, B. M. Jun, J. R. V. Flora, et al., Chemosphere **229**, 142–159 (2019). https://doi.org/10.1016/j.chemosphere.2019.04.198
18. N. M. Livanova, E. S. Pravada, L. A. Kovaleva, et al., Russ. J. Phys. Chem. B **17**, 738–744 (2023). https://doi.org/10.1134/S1990793123030077
19. M. G. Kucherenko, P. P. Neyasov, and N. Y. Kruchinin, Russ. J. Phys. Chem. B **17**, 745–754 (2023). https://doi.org/10.1134/S1990793123030053
20. M. M. Avilova, N. V. Zolotareva, and O. V. Popova, Russ. J. Phys. Chem. B **17**, 329–335 (2023). https://doi.org/10.1134/S1990793123020203
21. F. Mollaamin and M. Monajjemi, J. Carbon Res. C **9** (2), 61 (2023). doi
22. A. K. Gatin, S. Y. Sarvadiy, N. V. Dokhlikova, et al., J. Phys. Chem. B **15**, 367–372 (2021). https://doi.org/10.1134/S1990793121030209
23. M. Jeon, B. M. Jun, S. Kim, et al., Chemosphere **261**, 127781 (2020). https://doi.org/10.1016/j.chemosphere.2020.127781
24. I. Ihsanullah, Chemosphere **263**, 127970 (2021). https://doi.org/10.1016/j.chemosphere.2020.127970
25. S. Bagheri, M. Monajjemi, A. Ziglari, et al., Russ. J. Phys. Chem. B **15** (Suppl. 1), S140–S148 (2021). https://doi.org/10.1134/S1990793121090049
26. D. Gonzalez-Ortiz, C. Salameh, M. Bechelany, et al., Mater. Today Adv. **8**, 100107 (2020). https://doi.org/10.1016/j.mtadv.2020.100107
27. F. Mollaamin and M. Monajjemi, Chemistry **5**, 365–380 (2023). https://doi.org/10.3390/chemistry5010027
28. A. A. Voznyakovsky, A. P. Wozniakovsky, S. V. Kidalov, et al., Russ. J. Phys. Chem. B **15**, 377–380 (2021). https://doi.org/10.1134/S1990793121030325
29. F. Mollaamin and M. Monajjemi, Computation **11**, 108 (2023). https://doi.org/10.3390/computation11060108
30. S. J. Pearton, B. S. Kang, S. K. Kim, et al., J. Phys. Condens. Matter **16**, R961–R994 (2004). https://doi.org/10.1088/0953-8984/16/29/R02
31. V. M. Volokhov, T. S. Zyubina, A. V. Volokhov, et al., Russ. J. Phys. Chem. B **15**, 12–24 (2021). https://doi.org/10.1134/S1990793121010127
32. F. Mollaamin, M. Monajjemi, S. Salemi, et al., Fuller. Nanotub. Carbon Nanostructures **19**, 182–196 (2011). https://doi.org/10.1080/15363831003782932
33. R. Jha, A. Singh, P.K. Sharma, et al., J. Drug Deliv. Sci. Technol. **58**, 101811 (2020). https://doi.org/10.1016/j.jddst.2020.101811
34. M. Monajjemi, M. Khaleghian, N. Tadayonpour, et al., Int. J. Nanosci. **9**, 517–529 (2010). https://doi.org/10.1142/S0219581X10007071
35. F. Mollaamin, Computation **11** (4), 84 (2023). https://doi.org/10.3390/computation11040084
36. H. Cui, Y. Yong, H. Jiang, et al., Mater. Res. Express **4**, 015009 (2017). https://doi.org/10.1088/2053-1591/aa56a9
37. Y. Yong, H. Jiang, X. Li, et al., Phys. Chem. Chem. Phys. **18**, 21431–21441 (2016). https://doi.org/10.1039/C6CP02931K

38. K. H. Baik, J. Kim, and S. Jang, Sens. Actuators B **238**, 462–467 (2017). https://doi.org/10.1016/j.snb.2016.07.091
39. Y. Yong, H. Cui, Q. Zhou, et al., RSC Adv. **7**, 51027–51035 (2017). https://doi.org/10.1039/c7ra11106a
40. M. A. H. Khan, Sensors **20**, 3889 (2020). https://doi.org/10.3390/s20143889
41. R. S. Bangari, V. K. Yadav, J. K. Singh, et al., ACS Omega **5** (18), 10301–10314 (2020). https://doi.org/10.1021/acsomega.9b04295
42. Y. H. Chao, J. Zhang, H.P. Li, et al., Chem. Eng. J. **387**, 124138 (2020). https://doi.org/10.1016/j.cej.2020.124138
43. Y. Guo, R. X. Wang, P. F. Wang, et al., ACS Sustain. Chem. **7** (6), 5727–5741 (2019). https://doi.org/10.1021/acssuschemeng.8b05150
44. V. Sharma, H. L. Kagdada, P. K. Jha, et al., Renewable Sustainable Energy Rev. **120**, 109622 (2020). https://doi.org/10.1016/j.rser.2019.109622
45. S. Mateti, I. Sultana, Y. Chen, et al., Batteries **9**, 344 (2023). https://doi.org/10.3390/batteries9070344
46. Y. Zhang, H. Si, S. Liu, et al., J. Alloys Compd. **850**, 156680 (2020). https://doi.org/10.1016/j.jallcom.2020.156680
47. Y.-G. Park, S.-N. Nam, M. Jang, et al., Sep. Purif. Technol. **288**, 120637 (2022). https://doi.org/10.1016/j.seppur.2022.120637
48. N. M. Livanova, V. A. Hasova, E. S. Pravada, et al., Russ. J. Phys. Chem. B **16**, 756–763 (2022). https://doi.org/10.1134/S1990793122040108
49. D. V. Shtansky, A. T. Matveev, E. S. Permyakova, et al., Nanomaterials **12**, 2810 (2022). https://doi.org/10.3390/nano12162810
50. Y. Yang, Y. Peng, M. F. Saleem, et al., Materials **15**, 4396 (2022). https://doi.org/10.3390/ma15134396
51. A. Davies, J. D. Albar, A. Summerfield, et al., Nano Lett. **18**, 498–504 (2018). https://doi.org/10.1021/acs.nanolett.7b04453
52. R. Dennington, T. A. Keith, and J. M. Millam, *GaussView. Version 6* (Semichem Inc., Shawnee Mission, KS, 2016).
53. M. J. Frisch, G. W. Trucks, H. B. Schlegel, G. E. Scuseria, M. A. Robb, J. R. Cheeseman, G. Scalmani, V. Barone, G. A. Petersson, H. Nakatsuji, X. Li, M. Caricato, A. V. Marenich, J. Bloino, B. G. Janesko, R. Gomperts, B. Mennucci, H. P. Hratchian, J. V. Ortiz, A. F. Izmaylov, J. L. Sonnenberg, D. Williams-Young, F. Ding, F. Lipparini, F. Egidi, J. Goings, B. Peng, A. Petrone, T. Henderson, D. Ranasinghe, V. G. Zakrzewski, J. Gao, N. Rega, G. Zheng, W. Liang, M. Hada, M. Ehara, K. Toyota, R. Fukuda, J. Hasegawa, M. Ishida, T. Nakajima, Y. Honda, O. Kitao, H. Nakai, T. Vreven, K. Throssell, J. A. Montgomery, Jr., J. E. Peralta, F. Ogliaro, M. J. Bearpark, J. J. Heyd, E. N. Brothers, K. N. Kudin, V. N. Staroverov, T. A. Keith, R. Kobayashi, J. Normand, K. Raghavachari, A. P. Rendell, J. C. Burant, S. S. Iyengar, J. Tomasi, M. Cossi, J. M. Millam, M. Klene, C. Adamo, R. Cammi, J. W. Ochterski, R. L. Martin, K. Morokuma, O. Farkas, J. B. Foresman, and D. J. Fox, *Gaussian 16, Revision C.01* (Gaussian, Inc., Wallingford, CT, 2016).
54. J. P. Perdew, K. Burke, M. Ernzerhof, Phys. Rev. Lett. **77**, 3865 (1996). https://doi.org/10.1103/PhysRevLett.77.3865
55. F. Mollaamin, M. Monajjemi, J. Carbon Res. C **9** (1), 20 (2023). doi
56. Y. G. Zhou, X. T. Zu, F. Gao, et al., J. Appl. Phys. **105** (10), 104311 (2009). https://doi.org/10.1063/1.3130401
57. Y. Mao, J. Yuan, and J. Zhong, J. Phys.: Condens. Matter **20** (11), 115209 (2008). https://doi.org/10.1088/0953-8984/20/11/115209
58. F. Mollaamin and M. Monajjemi, Clean Technol. **5** (1), 403–417 (2023). https://doi.org/10.3390/cleantechnol5010020
59. M. Monajjemi, F. Mollaamin, M.R. Gholami, et al., Main Group Met. Chem. **26**, 349–362 (2003). https://doi.org/10.1515/MGMC.2003.26.6.349
60. F. Mollaamin, S. Shahriari, M. Monajjemi, et al., J. Clust. Sci. **34**, 1547–1562 (2023). https://doi.org/10.1007/s10876-022-02335-1
61. M. Monajjemi, F. Mollaamin, and S. Shojaei, Biointerface Res. Appl. Chem. **3**, 5575–5585 (2020). https://doi.org/10.33263/BRIAC103.575585
62. F. Mollaamin and M. Monajjemi, J. Mol. Model. **29**, 119 (2023). https://doi.org/10.1007/s00894-023-05526-3
63. X. Miao, S. Zhou, and C. Wang, Russ. J. Phys. Chem. B **16**, 804–808 (2022). https://doi.org/10.1134/S199079312204011X
64. F. Mollaamin and M. Monajjemi, Mol. Simul. **49** (4), 365–376 (2023). https://doi.org/10.1080/08927022.2022.2159996
65. M. A. A. Zadeh, H. Lari, L. Kharghanian, et al., J. Comput. Theor. Nanosci. **12**, 4358–4367 (2015). https://doi.org/10.1166/jctn.2015.4366
66. F. Mollaamin and M. Monajjemi, J. Bio Tribo Corros. **9**, 33 (2023). doi
67. Y. Takeshi, D. P. Tew, and N. C. Handy, Chem. Phys. Lett. **393** (1–3), 51–57 (2004). https://doi.org/10.1016/j.cplett.2004.06.011
68. S. Lehtola, Int. J. Quantum Chem. **119**, e25968 (2019). https://doi.org/10.1002/qua.25968
69. L. S. Shibryaeva, L. R. Lyusova, S. G. Karpova, et al., Russ. J. Phys. Chem. B **16**, 334–345 (2022). https://doi.org/10.1134/S199079312202021X
70. E. A. Lebedeva, S. A. Astaf'eva, and T. S. Istomina, Russ. J. Phys. Chem. B **16**, 316–322 (2022). https://doi.org/10.1134/S1990793122010109
71. V. G. Kytin, V. G. Duvakina, and E. A. Konstantinova, et al., Russ. J. Phys. Chem. B **16**, 421–425 (2022). https://doi.org/10.1134/S1990793122030186
72. H. A. Young and R. D. Freedman, *Sears and Zemansky's University Physics with Modern Physics*, 13th ed. (Addison-Wesley, Boston, 2012), p. 754.
73. K. Bakhshi, F. Mollaamin, M. Monajjemi, J. Comput. Theor. Nanosci. **8**, 763–768 (2011). https://doi.org/10.1166/jctn.2011.1750

74. F. Mollaamin, A. Ilkhani, N. Sakhaei, et al., J. Comput. Theor. Nanosci. **12**, 3148–3154 (2015). https://doi.org/10.1166/jctn.2015.4092
75. B. Khalili Hadad, F. Mollaamin, and M. Monajjemi, Russ. Chem. Bull. **60**, 238–241 (2011). https://doi.org/10.1007/s11172-011-0039-5
76. M. Monajjemi, M. T. Baie, and F. Mollaamin, Russ. Chem. Bull. **59**, 886–889 (2010). https://doi.org/10.1007/s11172-010-0181-5
77. F. Mollaamin and M. Monajjemi, Surf. Rev. Lett. (2023). https://doi.org/10.1142/S0218625X24500057
78. A. Tahan, F. Mollaamin, and M. Monajjemi, Russ. J. Phys. Chem. A **83**, 587–597 (2009). https://doi.org/10.1134/S003602440904013X
79. F. Mollaamin and M. Monajjemi, J. Clust. Sci. **34**, 2901–2918 (2023). https://doi.org/10.1007/s10876-023-02436-5
80. E. M. Sarasia, S. Afsharnezhad, B. Honarparvar, et al., Phys. Chem. Liq. **49**, 561–571 (2011). https://doi.org/10.1080/00319101003698992
81. F. Mollaamin, M. Monajjemi, J. Mol. Model. **29**, 170 (2023). https://doi.org/10.1007/s00894-023-05567-8
82. B. Ghalandari, M. Monajjemi, and F. Mollaamin, J. Comput. Theor. Nanosci. **8**, 1212–1219 (2011). https://doi.org/10.1166/jctn.2011.1801
83. F. Mollaamin, and M. Monajjemi, Sensor Rev. **43** (4), 266–279 (2023). https://doi.org/10.1108/SR-03-2023-0040
84. M. Khaleghian, M. Zahmatkesh, F. Mollaamin, et al., Fuller. Nanotub. Carbon Nanostruct. **19**, 251–261 (2011). https://doi.org/10.1080/15363831003721757
85. F. Mollaamin, M. Monajjemi, J. Bio Tribo Corros. **9**, 47 (2023). doi